A criterion to assess the relevance of structural flexibility on the seismic response of large buried structures [*]

Ariel Santana, Juan J. Aznárez, Luis A. Padrón and Orlando Maeso

Instituto Universitario de Sistemas Inteligentes y Aplicaciones Numéricas en Ingeniería (SIANI)
Universidad de Las Palmas de Gran Canaria, 35017 Las Palmas de Gran Canaria, Spain

Abstract

This paper analyzes the requirements of the models needed to estimate the seismic motions observed along large cylindrical buried structures by performing a parametric analysis of the problem using two different models: one in which the buried structure is considered as perfectly rigid, and another one in which its actual structural flexibility is taken into account. The study is performed using a Beam-on-Dynamic-Winkler-Foundation approach, and the models are previously verified by comparison against results obtained for the problem at hand using a more rigorous 3D multidomain boundary element model. The results obtained by comparison of the seismic responses estimated by both models are used to build and propose a specific criterion that can be used to elucidate under which circumstances is it possible to neglect the structural flexibility. It is found that, contrary to what is commonly assumed, the structural slenderness ratio alone cannot be used, in general, to predict the validity of the rigid structure approach: embedment lengths, soil stiffness, depth of interest and natural period of study are, also, key parameters that need to be taken into account. A close-form criterion, is proposed in table form taking all such parameters into account.

Keywords: buried structures, seismic response, structural flexibility, design criterion

1 Introduction

Assessing the motions arising at different points within buried structures due to the action of incoming seismic waves may be needed when such structures are due to house sensitive equipment such as instruments, turbines, pumps, etc. In many occasions, the systems under study are big massive structures. Therefore, when setting up a model for studying these motions of seismic origin within the structure, one aspect to consider is whether it is really needed to take into account its actual structural flexibility or, on the contrary, a perfectly rigid representation of it is enough, mainly in cases of stout, non-slender configurations. It might be tempting to consider those large non-slender structures as perfectly rigid in relationship with the surrounding soil. The kinematic response of an actual structure of that kind is studied for instance in Vega et al. [32], where differences between rigid and flexible approaches are quantified and, even though the structure was non-slender and, apparently, very rigid, the rigid and flexible models provided results with important discrepancies, observation which provided motivation for the present piece of research.

With a few exceptions related to the impedance problem (see e.g. Saitoh and Watanabe [25]), the available literature on the topic does not include proposals of well-founded general criteria for making this kind of decision. For this reason, this paper contributes to this issue by presenting a

criterion that can be used for practical purposes by structural and geotechnical engineers to establish if a structure under seismic excitation can be considered as a rigid body or, on the contrary, its real flexibility can not be neglected. The criterion is based on a parametric analysis that studies the errors between the motions of seismic origin provided by two models in which the buried structure is considered from both points of view (perfectly rigid or with its actual flexiblity).

In this respect, this parametric analysis is performed using Beam-on-Dynamic-Winkler-Foundation (BDWF) approaches, previously verified by comparison against results obtained for the problem at hand using a more rigorous 3D multidomain boundary element model [16, 17]. These BDWF approaches follow the line of previous works related to the dynamic analysis of piles (Flores-Berrones and Whitman [8]; Gazetas and Dobry [9]; Kavvadas and Gazetas [14] or Mylonakis [21]) or rigid foundations (Gerolymos and Gazetas [10] and Varun et al. [31]). These are very well known models in which the structure is modeled as a beam, and the surrounding soil is represented through unconnected springs and dashpots distributed along its buried length. One of the main differences between such models lies in the way to establish the properties of those springs and dashpots. In this sense, most BDWF models found in the literature could be classified in the following two groups: a) models that adjust those properties based on numerical models that take into account the actual nature of the problem (see e.g. Makris and Gazetas [19]; Makris [18] or Kavvadas and Gazetas [14]) and b) models that propose those values based on theoretical wave propagation approaches as closed-form functions in the frequency domain, as in the work of Baranov-Novak [22] who develop an elastodynamic plain–strain approach, assuming that the soil is divided in an infinite number of independent thin horizontal slices, and provide a simplified formulation of stress field in soil. The classic expression provided by Novak et al. [23], that are also part of this second group, will be the one used in the models presented herein. Finally, we can not fail to mention the existence of other more evolved analytic models formulated as solutions of the three–dimensional problem (Tajimi [28]). In this sense, the works of Mylonakis [20], Anoyatis and Lemnitzer [1] or Bahrami and Nikraz [3] are very interesting.

The specific problem addressed in this work is one corresponding to a cylindrical structure (hollow or solid) embedded in a half–space. The study has been carried out using a wide range of properties for both, structure and soil. Taking into account the embedded length of the structures included in this analysis, the hypothesis of a homogeneous half–space to model the ground may be unrealistic in some practical problems. Thus, this work should be understood as a first approach to the problem that has the purpose of provide a simple engineering criterion in order to be able to discern under which circumstances it is realistic to assume a rigid seismic behaviour of the structure. In that case, it will be possible the use of, e.g., calibrated Winkler models in the line of the mentioned Gerolymos and Gazetas [10] or Varun et al. [31], or well established response functions for perfectly rigid structures (such as, for instance, those provided by the classic works of Elsabee et al. [6] or Kausel et al. [13] and more recently Conti et al. [5]), without the need of using more rigorous and sophisticated models, in the line of continuum–base approaches as the ones used, for example, for the analysis of the seismic response of tunnels [11, 24, 12, 15, 2], or for the seismic analysis of real pumping structures, as the aforementioned Vega et al. [32].

This paper is structured as follows. After the introduction, the problem at hand is presented in section 2, as well as the key aspects and parameters that affect the seismic response of the system. The methodology and the BDWF models formulation, are explained in section 3. Section 4 includes validation results of the BDWF models against a more rigorous 3D multidomain boundary element model. Finally, results and the criterion proposed are included in section 5, followed by conclusions in section 6.

2 Problem description

In order to look into the influence of the structural flexibility on the seismic response of large buried structures, the results of two different models, that consider the structure either as a flexible solid or as an infinitely rigid body, are compared and analyzed (see Figure 1).

The structure is idealized geometrically as a completely buried solid cylinder of diameter D or a cylindrical shell with constant outer and inner diameters D and D_{int}, and length L. The type of section will be specified by a parameter $\delta = D_{int}/D$ defining a hollow $(0 < \delta < 1)$ or solid $(\delta = 0)$ cross section. Welded contact conditions are assumed at the interface between the structure and the surrounding soil, which is assumed to be a isotropic and homogenous half–space with Poisson's ratio ν_s, density ρ_s and shear wave velocity V_s. The system, for which a linear–elastic behaviour is assumed, is subjected to vertically–incident shear waves.
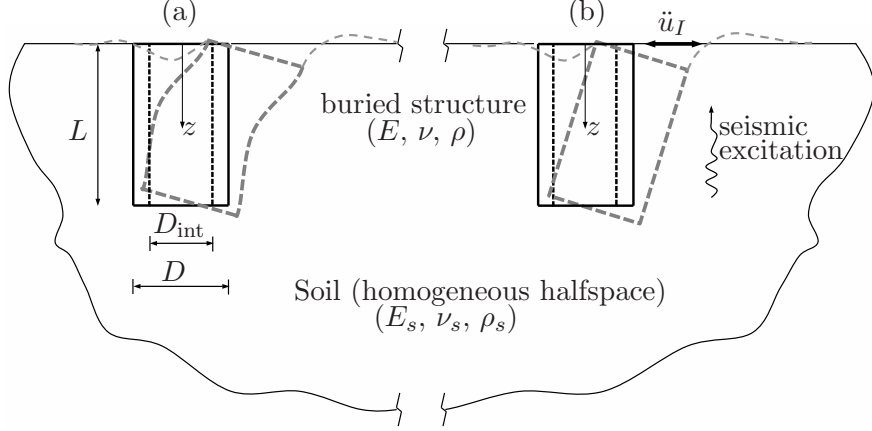

Figure 1: Problem description. Influence of the structural flexibility on the seismic response of large structures buried in homogeneous soil. (a) Deformable solid approach, (b) Rigid body approach

The properties of the soil, the flexibility of the structure and the variability of the seismic incident field along the buried length of the structure are three key aspects that affect the seismic response of the system. In this study, the flexibility of the structure depends on the type of cross section (solid or hollow), the material properties, and the slenderness ratio. The variability of the incident field, on the other hand, is related to the soil wave velocity (or soil stiffness) and the characteristics of the seismic waves. Thus, the study will be performed varying the following four parameters of the problem: a) Type of structural cross section: hollow $(\delta = 0.85)$ or solid $(\delta = 0.00)$; b) Slenderness ratio of the structure $(L/D = 2 - 10)$; c) Soil shear wave velocity $(V_s = 200 - 1000 \, \text{m/s}^2)$ and; d) Embedment lengths of the structure $(L = 20, 40, 60 \text{ and } 80 \, \text{m})$.

The rest of properties, considered as non–relevant for the aim of this study, are kept constant. The structure is assumed to be made in concrete, characterized by its Young's modulus $E = 2.76 \cdot 10^{10} \, \text{N/m}^2$, Poisson's ratio $\nu = 0.2$ and density $\rho = 2500 \, \text{kg/m}^3$. On the other hand, Poisson's ratio $\nu_s = 0.3$ and density $\rho_s = 1570 \, \text{kg/m}^3$ are kept constant for the soil. With all this, the resultant relationships between structural concrete and soil stiffnesses at the limits of the scopes defining each ground type are also presented in Table 1. A wide range of values for the ratio E/E_s is covered, going from below 3 for ground type A to over 200 for ground type D.

The range of soil properties given above covers Eurocode–8 [7] ground types A, B, C and D. The vertically–incident SH wavefield that impinges the system generates free–field ground surface accelerations compatible with the type 1 design elastic horizontal ground motion acceleration response spectra also provided by Eurocode–8 [7] for each ground type. Therefore, different synthetic accelerograms, one for each ground type, are used as excitation motion according to the shear wave velocity defining the soil in each configuration.

The response will be studied in terms of accelerations measured at five points with different depths along the structure, $z/L = 0.00$ (top of the structure), 0.25, 0.50, 0.75 and 1.00 (bottom of the structure). The main objective is presenting a criterion to decide when is the hypothesis of infinite rigidity valid for a large buried structure. Therefore, the results need to be synthesized and presented in terms of the deviation of the response obtained from the rigid body assumption

Table 1: Relationships between structural concrete and soil stiffnesses at the limits of the scopes defining each ground type

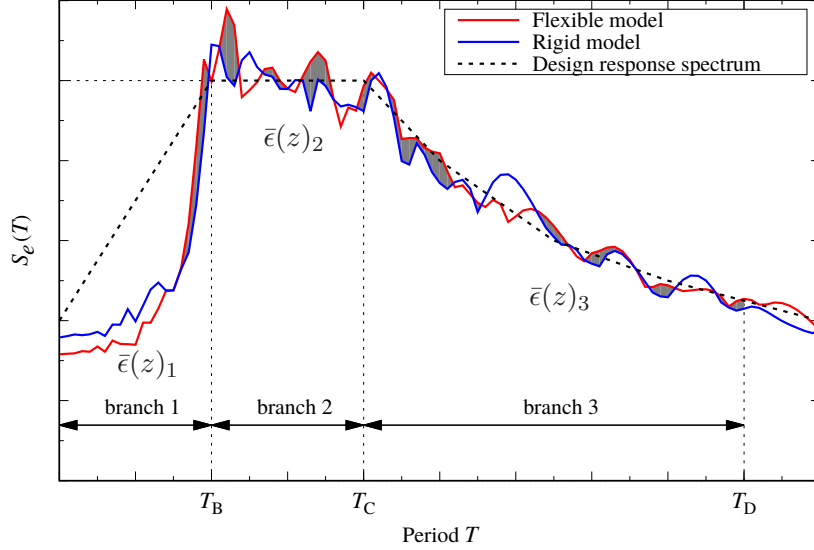| Ground type	V_s (m/s)	E_s (N/m^2)	E/E_s
A	1500	$1.024 \cdot 10^{10}$	~ 3
	800	$2.912 \cdot 10^{9}$	~ 10
B	800	$2.912 \cdot 10^{9}$	~ 10
	360	$5.897 \cdot 10^{8}$	~ 50
C	360	$5.897 \cdot 10^{8}$	~ 50
	180	$1.474 \cdot 10^{8}$	~ 200
D	< 180	$< 1.474 \cdot 10^{8}$	> 200

Figure 2: Representation of average difference $\epsilon(z)_j$ (shaded area) between rigid body assumption and flexible response spectra along three branches defining the design response spectrum.

with respect to a flexible structure model. This deviation is defined as differences between the horizontal acceleration elastic response spectra characterizing the horizontal motions at different depths. These differences will be quantified in terms of average differences along every one of the three branches defining the elastic response spectra used (see figure 2). This average difference $\bar{\epsilon}(z)_j$ along branch j is defined as

$$\bar{\epsilon}(z)_j[\%] = \frac{1}{n_j} \sum_i^{n_j} \left| \frac{S_e^f(T_i,z) - S_e^r(T_i,z)}{S_e^r(T_i,z)} \right| \Psi_i \quad ; \quad j = \begin{cases} 1, T_i & / & T_i \leqslant T_B \\ 2, T_i & / & T_B \leqslant T_i \leqslant T_C \\ 3, T_i & / & T_C \leqslant T_i \leqslant 2 \end{cases} \quad (1)$$

where

$$\Psi_i = \frac{1 + \text{sign}\left(S_e^f(T_i,z) - S_e^r(T_i,z)\right)}{2} \times 100 \quad (2)$$

and n_j is the number of specific periods at which the elastic response spectrum is computed along branch j, while $S_e^r(T_i,z)$ and $S_e^f(T_i,z)$ are the elastic horizontal acceleration response spectra characterizing the horizontal motions of the embedded structure either as a perfectly rigid or flexible body, respectively. The values of the periods T_B and T_C depend on the ground type according to Eurocode–8 [7]. For the present study, the responses are always computed at 120 different periods distributed from $T = 0.01\,\text{s}$ to $T = 2\,\text{s}$. Note that errors are not added when

the solution provided by the rigid model is more conservative than that of the flexible one. The rotational motions along the structure are not taken into account when computing those elastic horizontal acceleration response spectra.

3   Methodology

Carrying out the wide parametric study established in the previous section involves computing the seismic response of a relatively large number of configurations of buried structures. This large set of analyses makes advisable the use of a numerical tool of low computational cost but accurate enough and able to adequately capture the differences arising when considering either a perfectly rigid or a flexible model for the buried structures. This is why the present study is carried out through the use of a frequency domain analysis procedure in which the frequency response functions (FRFs) for each case are computed by means of a linear–elastic model based on the Beam-on-Dynamic-Winkler-Foundation (BDWF) approach (see Figure 3), and the response of the system is then computed for a given seismic input signal compatible with the corresponding response spectrum.
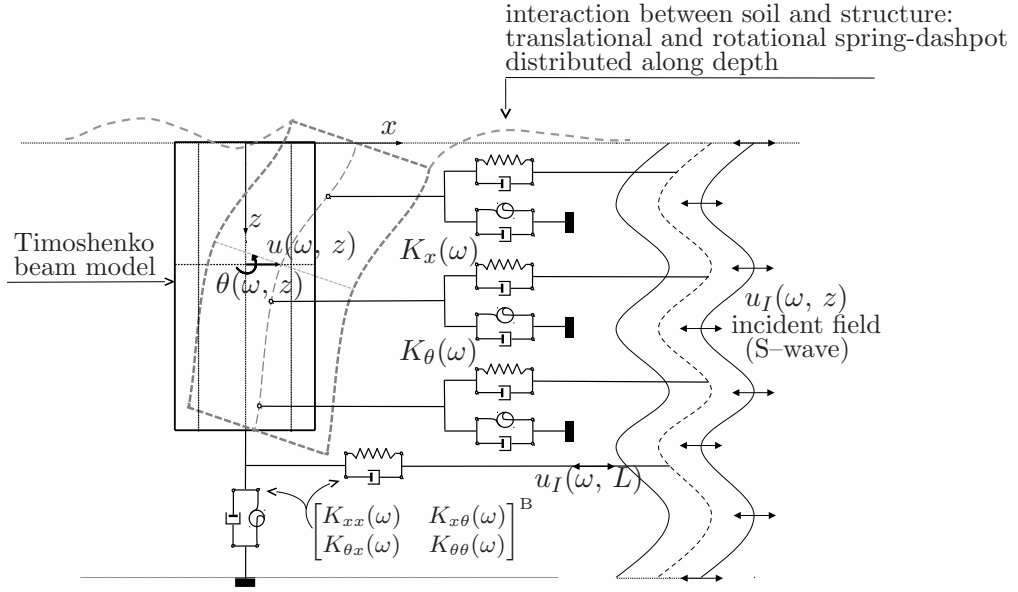

Figure 3: BDWF model for the analysis of KI response of flexible buried structure excited by vertical seismic shear wave

In order to be able to adequately represent the behaviour of the non-slender configurations, the Timoshenko beam formulation [29, 30], as part of a BDWF approach, is adopted in this work to model the buried structure. As mentioned above, the soil reactions to the lateral and rocking harmonic structural motions are modelled using the expressions of complex impedances proposed by Novak et al. [23]. These impedances relate the horizontal displacements $u = u(\omega, z)$ along the structural axis and the free–field displacement $u_I = u_I(\omega, z)$ produced by the vertically–incident SH wave field. Also, a moment over the structure is induced by this impedances and the rotation of the section of the structure $\theta(\omega, z)$.

3.1   BDWF Model Formulation

Taking rotatory inertia and shearing deformation into account, the governing equation that represents the transversal behaviour of the flexible structure according to this BDWF approach, can be written in the frequency domain as follows:

$$
\frac{\partial^4 u}{\partial z^4} - \left[\frac{1}{\kappa \mu A} \left(K_x - \rho A \omega^2 \right) + \frac{1}{EI} \left(K_\theta - \rho I \omega^2 \right) \right] \frac{\partial^2 u}{\partial z^2}
$$
$$
+ \frac{1}{\kappa \mu A} \left(K_x - \rho A \omega^2 \right) \frac{1}{EI} \left(K_\theta + \kappa \mu A - \rho I \omega^2 \right) u
$$
$$
= -\frac{1}{\kappa \mu A} K_x \frac{\partial^2 u_I}{\partial z^2} + \frac{1}{EI} \left(K_\theta + \kappa \mu A - \rho I \omega^2 \right) \frac{1}{\kappa \mu A} K_x u_I \quad (3)
$$

where the horizontal displacement associated with the incident field u_I (of unit value at free–field ground surface) is:

$$
u_I(\omega, z) = \frac{1}{2} \left(e^{\mathrm{i}kz} + e^{-\mathrm{i}kz} \right) \quad (4)
$$

being $k = \omega / \mathrm{V}_s$ the wave number, z the vertical coordinate that defines the depth from the free soil surface, ω the excitation frequency, i the imaginary unit, E, μ and ρ the Youngs, shear modulus and the density of the structure, A the area, I the moment of inertia and κ the shear correction factor of the section (0.5 for hollow and 0.9 for solid sections). K_x and K_θ represent the soil stiffness for horizontal and rocking vibrations. These impedances, key to model the Soil–Structure interaction phenomena taking place, are defined by factors of stiffness and damping both of them distributed along the buried depth of the structure. In this work, as mentioned previously, the expressions proposed by Novak et al. [23] are used to define K_x and K_θ. Using their notation, those functions can be expressed as follows (see Appendix A):

$$
K_x = \mu_s \left[S_x^r \left(a_o, \nu_s, \xi_s \right) + \mathrm{i}\, S_x^i \left(a_o, \nu_s, \xi_s \right) \right] \quad (5a)
$$
$$
K_\theta = \mu_s D^2 \left[S_\theta^r \left(a_o, \nu_s, \xi_s \right) + \mathrm{i}\, S_\theta^i \left(a_o, \nu_s, \xi_s \right) \right] \quad (5b)
$$

where μ_s, ν_s and ξ_s are the shear modulus, Poisson's ratio and damping ratio of surrounding soil and $a_o = \omega D / \mathrm{V}_s$ is the dimensionless frequency. At this point, it is useful to write the governing equations of the problem in a non–dimensional form. Following Vaschy-Buckingham's theory [4], it is easy to see that such equations can be written as functions of four dimensionless variables $(L/D, E/E_s, \rho/\rho_s, a_o)$ besides the five intrinsically dimensionless ratios involved (ν, δ, κ, ν_s, ξ_s). Thus, considering the vertical dimensionless coordinate $\xi = z/L$, the governing equation (3) can be written as:

$$
\frac{\partial^4 u}{\partial \xi^4} - \alpha \frac{\partial^2 u}{\partial \xi^2} + \beta\, u = -\gamma \frac{\partial^2 u_I}{\partial \xi^2} + \eta\, u_I \quad (6)
$$

where the dimensionless coefficients α, β, γ and η, for the present case of cylindrical structures, are defined as:

$$
\alpha = \alpha_1 + \alpha_2 \quad (7a)
$$
$$
\beta = \alpha_1 \alpha_2 + \alpha_1 \frac{\tilde{\alpha}_2}{\tilde{\alpha}_1} \left(\frac{L}{D} \right)^2 \quad (7b)
$$
$$
\gamma = \tilde{\alpha}_1 \left(S_x^r + \mathrm{i}\, S_x^i \right) \quad (7c)
$$
$$
\eta = \alpha_2 \gamma + \tilde{\alpha}_2 \left(S_x^r + \mathrm{i}\, S_x^i \right) \left(\frac{L}{D} \right)^2 \quad (7d)
$$

being

$$
\alpha_1 = \tilde{\alpha}_1 \left[\left(S_x^r + \mathrm{i}\, S_x^i \right) - \frac{\pi}{4} a_o^2 \frac{\rho}{\rho_s} \left(1 - \delta^2 \right) \right] \quad (8a)
$$
$$
\alpha_2 = \tilde{\alpha}_2 \left[\left(S_\theta^r + \mathrm{i}\, S_\theta^i \right) - \frac{\pi}{64} a_o^2 \frac{\rho}{\rho_s} \left(1 - \delta^4 \right) \right] \quad (8b)
$$

6

The constant $\tilde{\alpha}_1$ and $\tilde{\alpha}_2$ included in these expressions are:

$$\tilde{\alpha}_1 = \frac{4}{\pi}\frac{1}{\kappa}\frac{1+\nu}{1+\nu_s}\frac{E_s}{E}\left(\frac{L}{D}\right)^2\frac{1}{1-\delta^2} \quad ; \quad \tilde{\alpha}_2 = \frac{32}{\pi}\frac{1}{1+\nu_s}\frac{E_s}{E}\left(\frac{L}{D}\right)^2\frac{1}{1-\delta^4} \tag{9}$$

The general solution for the displacements along the beam that verifies eq. (6) has the form:

$$u\left(\xi,\omega\right) = C_1\,e^{s_1\xi} + C_2\,e^{s_2\xi} + C_3\,e^{s_3\xi} + C_4\,e^{s_4\xi} + C_p\left(e^{\mathrm{i}\lambda\xi} + e^{-\mathrm{i}\lambda\xi}\right) \tag{10}$$

where s_j are the solutions of the characteristic equation of the homogeneous problem:

$$s_j = \pm\left[\frac{\alpha}{2} \pm \frac{1}{2}\left(\alpha^2 - 4\beta\right)^{\frac{1}{2}}\right]^{\frac{1}{2}} \quad ; \quad j = 1,2,3,4 \tag{11}$$

and C_p is the amplitude corresponding to the particular solution that represent the behaviour related to dynamic loading (incident wave) proposed:

$$C_p = \frac{\Delta}{\lambda^4 + \alpha\lambda^2 + \beta} \quad ; \quad \Delta = \frac{1}{2}\left[a_o^2\left(\frac{L}{D}\right)^2\gamma + \eta\right] \tag{12}$$

with

$$\lambda = \frac{a_o}{\sqrt{1 + 2\xi_s\mathrm{i}}}\left(\frac{L}{D}\right) \tag{13}$$

a dimensionless parameter related to the incident field wave number.

The amplitudes of the homogeneous solutions C_j in equation (10) are computed by imposing the boundary conditions at the top and bottom of the structure. Such equations are defined in terms of the bending moment $M\left(\xi,a_o\right)$ and shear force $Q\left(\xi,a_o\right)$ that, for the beam theory used in present approach, can be written in dimensionless form as:

$$\frac{ML^2}{EI} = \frac{\partial^2 u}{\partial\xi^2} - \alpha_1\,u + \gamma\,u_I \tag{14a}$$

$$\frac{QL^3}{EI} = \frac{1}{\phi}\left[\frac{\partial u}{\partial\xi} - (\theta L)\right] \tag{14b}$$

where $\theta\left(\xi,a_o\right)$ is the rotation of the beam cross–section and can be written as:

$$\theta L = \frac{1}{\alpha_3}\left[\frac{\partial u}{\partial\xi} + \phi\left(\frac{\partial^3 u}{\partial^3\xi} - \alpha_1\frac{\partial u}{\partial\xi} + \gamma\frac{\partial u_I}{\partial\xi}\right)\right] \tag{15}$$

in which

$$\phi = \frac{EI}{L^2\kappa\mu A} = \frac{1}{8}\frac{1}{\kappa}\left(\frac{L}{D}\right)^{-2}(1+\nu)(1+\delta^2) \tag{16a}$$

$$\alpha_3 = \tilde{\alpha}_1\left(\frac{L}{D}\right)^{-2}\left[\left(S_\theta^r + \mathrm{i}\,S_\theta^i\right) - \frac{\pi}{64}a_o^2\frac{\rho}{\rho_s}\left(1-\delta^4\right)\right] + 1 \tag{16b}$$

In the present problem, free condition are assumed at the top of structure ($\xi = 0$):

$$\left(\tilde{M}\right)^{\xi=0} = \left(\frac{ML^2}{EI}\right)^{\xi=0} = 0 \tag{17a}$$

$$\left(\tilde{Q}\right)^{\xi=0} = \left(\frac{QL^3}{EI}\right)^{\xi=0} = 0 \tag{17b}$$

7

while in the bottom ($\xi = 1$), the soil reactions are assumed to be related to the horizontal and rotational motions of the structure through an impedance matrix of the type

$$\begin{Bmatrix} Q \\ M \end{Bmatrix}^{\xi=1} + \begin{bmatrix} K_{xx} & K_{x\theta} \\ K_{\theta x} & K_{\theta\theta} \end{bmatrix}^B \begin{Bmatrix} u - u_I \\ \theta \end{Bmatrix}^{\xi=1} = \begin{Bmatrix} 0 \\ 0 \end{Bmatrix} \tag{18}$$

There exist a high uncertainty about the actual values of these bottom impedance functions, and little references can be found in the BDWF–related literature. In the present work, and in line with some recent works (see e.g. [27]), complex impedance functions corresponding to shallow rigid circular footing on a halfspace problem are adopted. As usual, the can be written as

$$K_{xx}^B (a_o, \nu_s) = \mu_s D \, \tilde{K}_x (a_o, \nu_s) \tag{19a}$$

$$K_{\theta\theta}^B (a_o, \nu_s) = \mu_s D^3 \, \tilde{K}_\theta (a_o, \nu_s) \tag{19b}$$

$$K_{x\theta}^B (a_o, \nu_s) = K_{\theta x}^B (a_o, \nu_s) = 0 \tag{19c}$$

In the present work, $\tilde{K}_{xx}$ and $\tilde{K}_{\theta\theta}$ are calculated from the closed-form solutions proposed by Veletsos and Verbič [33] (see Appendix B). Finally, after rearranging eq. (18) and using the problem dimensionless parameters, this equation can be written as

$$\left(\tilde{Q} \right)^{\xi=1} + \varphi_1 \, \tilde{K}_x \, (u - u_I)^{\xi=1} = 0 \tag{20a}$$

$$\left(\tilde{M} \right)^{\xi=1} + \varphi_2 \, \tilde{K}_\theta \, (\theta L)^{\xi=1} = 0 \tag{20b}$$

where

$$\varphi_1 = \frac{32}{\pi} \frac{1}{1 + \nu_s} \frac{E_s}{E} \left(\frac{L}{D} \right)^3 \quad ; \quad \varphi_2 = \frac{32}{\pi} \frac{1}{1 + \nu_s} \frac{E_s}{E} \left(\frac{L}{D} \right) \tag{21}$$

3.2 Winkler formulation for rigid model response

The frequency response functions corresponding to the model where the structure is assumed to be perfectly rigid can either be calculated by following a limiting process ($E/E_s \longrightarrow \infty$) from the BDWF model developed above; or directly by using rigid body dynamics. This last approach is very easy and leads to a 2×2 system of equations where the primary variables are the horizontal displacement of the center of gravity (G) $U_G(\omega)$ and the rocking rotation $\Theta_G(\omega)$ of structure (see Figure 4). From these variables, the kinematic equation for the horizontal displacements $u(\omega, z)$ at any location along the z-axis is

$$u(\omega, z) = U_G(\omega) - \Theta_G(\omega)(z - z_G) \tag{22}$$

In this approach, the dynamic equilibrium equations (force and moment equations) that govern the response of structure, can be formulated as follows:

$$K_x(\omega) \int_0^L [u_I(z, \omega) - u(z, \omega)] \, dz + K_{xx}^B(\omega) [u_I(L, \omega) - u(L, \omega)] = -\omega^2 M \, U_G(\omega) \tag{23a}$$

$$-K_\theta(\omega)\Theta_G(\omega)L - K_x(\omega) \int_0^L [u_I(z, \omega) - u(z, \omega)](z_G - z) \, dz - K_{\theta\theta}^B \Theta_G(\omega)$$
$$+K_{xx}^B(\omega)[u_I(L, \omega) - u(L, \omega)](L - z_G) = -\omega^2 I_G \, \Theta_G(\omega) \tag{23b}$$

where

$$M = \rho \frac{\pi}{4} D^2 \left(1 - \delta^2 \right) L \quad ; \quad I_G = \rho \frac{\pi}{16} D^2 \left(1 - \delta^2 \right) L \left[\frac{1}{4} D^2 \left(1 + \delta^2 \right) + \frac{1}{3} L^2 \right] \tag{24}$$
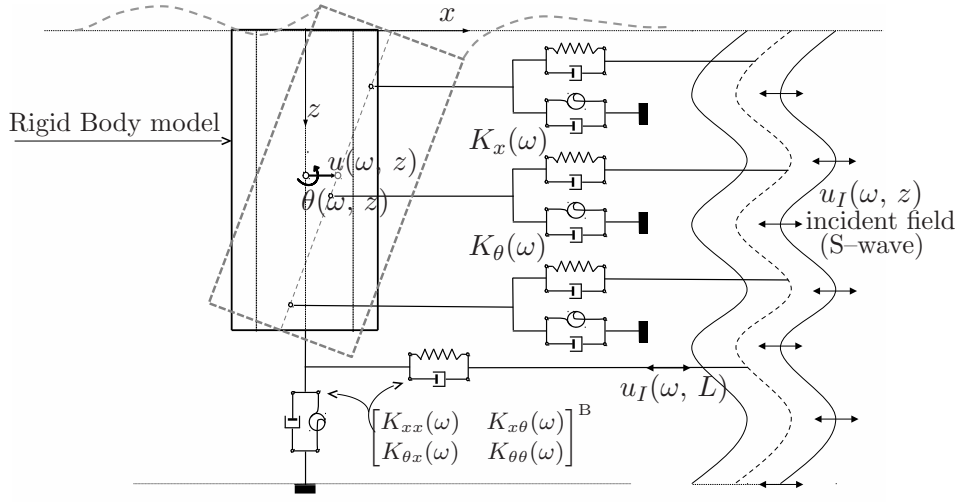
Figure 4: Representation of Winkler approach used in this study for the analysis of KI response of rigid buried structures under vertical seismic shear waves

are, respectively, the mass of structure and its rotational inertia about a transverse axis through G. Since the soil–structure interaction factors K_x, K_θ and K_{xx}^B, $K_{\theta\theta}^B$ are the same as in the flexible model, eq. (23) can be written, after some simple mathematical operations, as follows:

$$\begin{bmatrix} A_{11} & A_{12} \\ A_{21} & A_{22} \end{bmatrix} \begin{Bmatrix} U_G \\ \Theta_G D \end{Bmatrix} = \begin{Bmatrix} B_1 \\ B_2 \end{Bmatrix} \tag{25}$$

with

$$A_{11} = \frac{\pi}{4} a_o^2 \left(1 - \delta^2\right) \frac{\rho}{\rho_s} - \left(S_x^r + \mathrm{i}\, S_x^i\right) - \tilde{K}_x \left(\frac{L}{D}\right)^{-1} \tag{26a}$$

$$A_{12} = \left(S_x^r + \mathrm{i}\, S_x^i\right) \left(\xi_G - \frac{1}{2}\right) \frac{L}{D} + \tilde{K}_x \left(\xi_G - 1\right) \tag{26b}$$

$$A_{22} = \frac{\pi}{16} a_o^2 \left(1 - \delta^2\right) \left[\frac{1}{4}\left(1 - \delta^2\right) + \frac{1}{3}\left(\frac{L}{D}\right)^2\right] + \left(S_x^r + \mathrm{i}\, S_x^i\right) \left(\frac{L}{D}\right)^2 \left[\xi_G\left(1 - \xi_G\right) - \frac{1}{3}\right] \tag{26c}$$

$$- \left(S_\theta^r + \mathrm{i}\, S_\theta^i\right) - \tilde{K}_x \left(1 - \xi_G\right)^2 \frac{L}{D} - \tilde{K}_\theta \left(\frac{L}{D}\right)^{-1}$$

$$A_{21} = A_{12} \tag{26d}$$

$$B_1 = -\frac{1}{2} \left(S_x^r + \mathrm{i}\, S_x^i\right) \frac{1}{\mathrm{i}\lambda} \left(e^{\mathrm{i}\lambda} - e^{-\mathrm{i}\lambda}\right) - \frac{1}{2} \tilde{K}_x \left(e^{\mathrm{i}\lambda} + e^{-\mathrm{i}\lambda}\right) \left(\frac{L}{D}\right)^{-1} \tag{26e}$$

$$B_2 = \frac{1}{2} \left(S_x^r + \mathrm{i}\, S_x^i\right) \frac{1}{\mathrm{i}\lambda} \left(e^{\mathrm{i}\lambda} + e^{-\mathrm{i}\lambda}\right) \left(1 - \xi_G\right) \frac{L}{D}$$

$$+ \frac{1}{2} \left(S_x^r + \mathrm{i}\, S_x^i\right) \frac{1}{\lambda^2} \left(e^{\mathrm{i}\lambda} + e^{-\mathrm{i}\lambda} - 2\right) \frac{L}{D} - \frac{1}{2} \tilde{K}_x \left(e^{\mathrm{i}\lambda} + e^{-\mathrm{i}\lambda}\right) \left(1 - \xi_G\right) \tag{26f}$$

where all these coefficients are written in terms of dimensionless parameters (L/D, ρ/ρ_s, a_o, δ, ν_s, ξ_s) necessary to describe the problem in this case.

4   Verification

Before performing the parametric analysis described above, the formulations derived in section 3.1 for the flexible BDWF model and in section 3.2 for the rigid model are herein verified by

9

comparison against more rigorous continuum–type numerical solutions based on the Boundary Elements Method. To do this, a three–dimensional multidomain boundary element code developed by the authors [16, 17] is used as a reference solution, both for the flexible structure problem and for the rigid structure problem, case for which a specific formulation for the perfectly rigid structure hypothesis is even more suitable [26].

Comparisons are made for two representative cases within the ranges specified in section 2 for the parameters used in the present study: $L = 60$ m, $V_s = 500$ m/s, $L/D = 3$ and 8, and a solid cross section. Thus, figures 5 and 6 show the horizontal accelerations $a(t)$ [m/s^2] at the five points along the structure mentioned above (depths $z/L = 0.00$, 0.25, 0.50, 0.75 and 1.00). These accelerations are computed using the flexible and rigid BDWF formulations, respectively, and are compared with the results from the BEM model. It can be seen that the results, in general, show a good agreement.
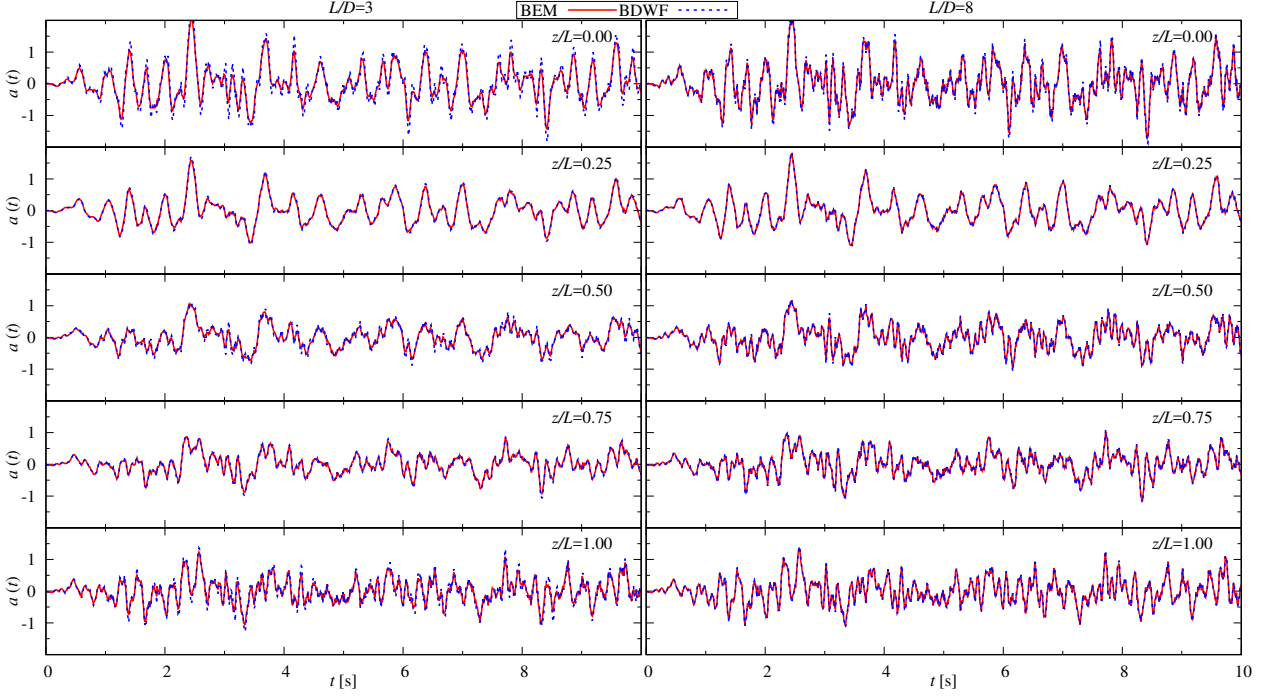

Figure 5: Actual flexibility assumption. Comparison between accelerations $a(t)$ [m/s^2] at different depths z/L of the buried structure computed with the BEM and Beam-on-Dynamic-Winkler models. $L = 60$ m, $V_s = 500$ m/s, $\delta = 0.0$, $L/D = 3$ (left) and 8 (right).

More importantly for this study, figures 7 and 8 present verification results in terms of the response spectra, where the differences related to the methodology are more visible than in time acceleration response. As expected, the BDWF simplified models provide better results for the more slender structure ($L/D = 8$) than for the less slender. In both cases, the results provided by the BDWF simplified models are quite close to those provided by the more rigorous 3D BEM formulation, except for the top and bottom points and the less slender structure ($L/D = 3$) where the magnitude of the error reaches 20%. When there appear differences, the BDWF models provide a spectral response that is always higher than the one computed by the more rigorous 3D BEM formulation. In any case, it is worth noting that the tendency of both models is the same when shifting between the flexible and the rigid structure hypothesis, i.e, if the spectral response of the system according to the BEM formulation increases when changing from the flexible structure to the rigid structure, the response provided by the BDWF increases too, and in the proportion, and vice versa. Therefore, the simplified BDWF model is considered to be a valid tool for the parametric analysis proposed in this paper.
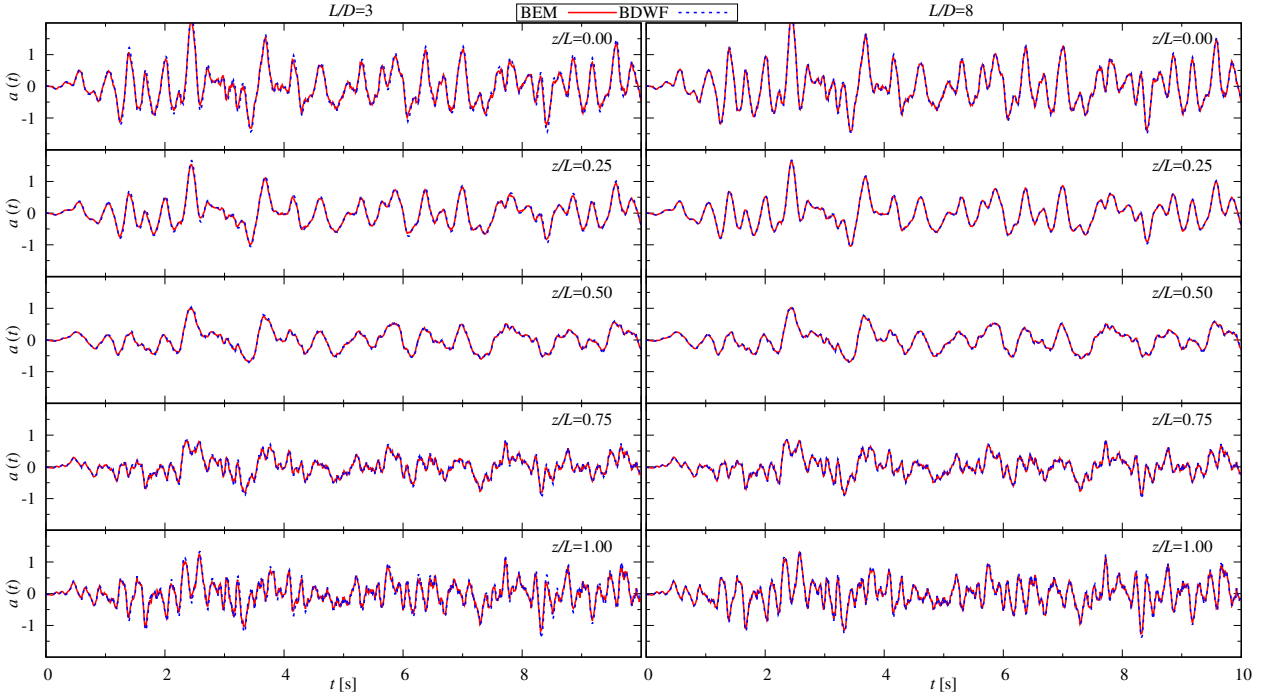
10

Figure 6: Rigid body assumption. Comparison between accelerations $a(t)$ [m/s^2] at different depths z/L of the buried structure computed with the BEM and Beam-on-Dynamic-Winkler models. $L = 60$ m, $V_s = 500$ m/s, $\delta = 0.0$, $L/D = 3$ (left) and 8 (right).
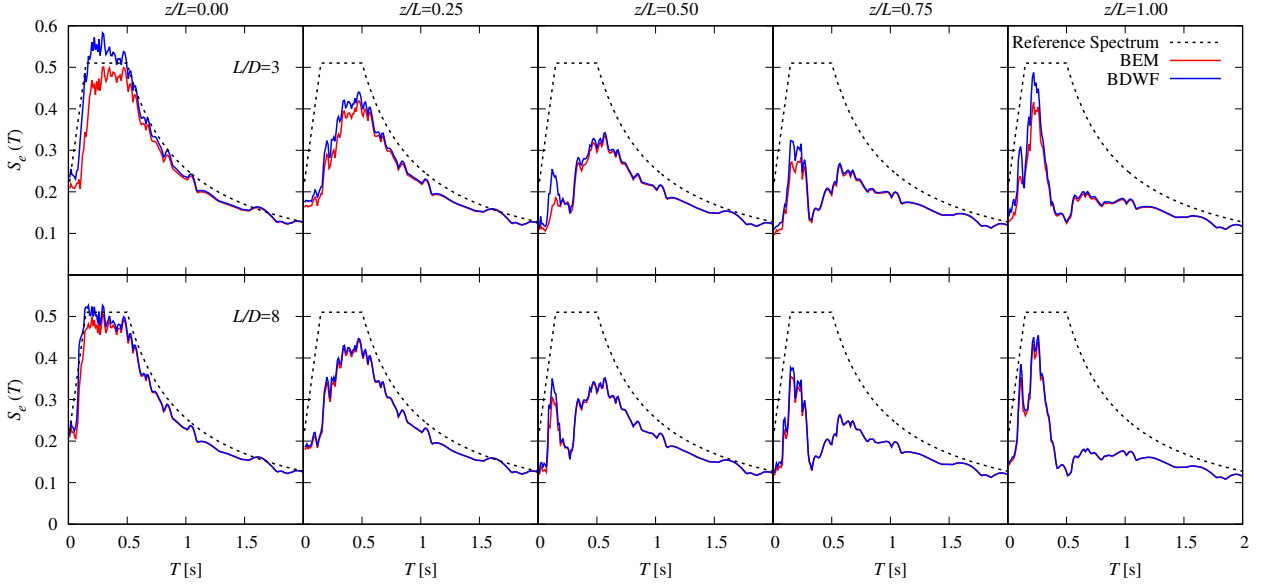

Figure 7: Actual flexibility assumption. Comparison between response spectra at different depths z/L of the buried structure computed with the BEM or Beam-on-Dynamic-Winkler models. $L = 60$ m, $V_s = 500$ m/s, $\delta = 0.0$, $L/D = 3$ (top) and 8 (bottom).

5 Results

The amount of results obtained from the parametric analysis described in section 2 is significantly large, and need to be synthesized in order to be useful to the principal aim of the present study, which is, as stated before, presenting a criterion to decide when is the hypothesis of infinity rigidity valid for a large buried structure subject to seismic action. First, a cut–off value for the average error (as defined in equation (1)) must be established as the maximum error for which the rigid
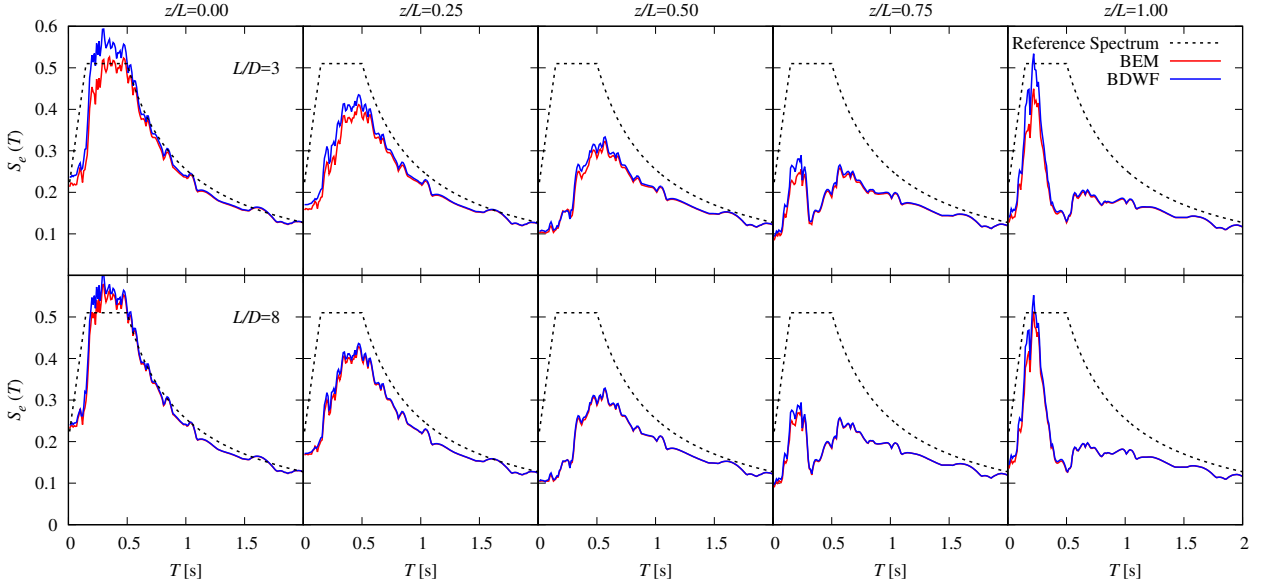
11

Figure 8: Rigid body assumption. Comparison between response spectra at different depths z/L of a buried structure obtained from the BEM or rigid Beam-On-Dynamic-Winkler models. $L = 60\,\text{m}$, $V_s = 500\,\text{m/s}$, $\delta = 0.0$, $L/D = 3$ (top) and 8 (bottom).

approach can still be considered adequate for the problem at hand. For practical applications, and taking into account the uncertainties associated to data and models, an average error below 10% is considered acceptable and is used as limit value to synthesize the results of the parametric analysis as described below.

Thus, figures 9 and 10, corresponding to hollow ($\delta = 0.85$) and solid structures, respectively, distinguishes the configurations (in terms of L/D and V_s values) for which the above-mentioned average differences $\bar{\epsilon}(z)$ are below or above 10%. More precisely, configurations for which $\bar{\epsilon}(z) > 10\%$ are those within the filled areas. Each figure contains two subsets of plots, the top one corresponding to the average differences computed along the low-periods branch of the response spectrum ($T_i \leqslant T_B$), and the bottom one corresponding to the intermediate-periods branch ($T_B \leqslant T_i \leqslant T_C$). Results for the high-periods branch ($T_C \leqslant T_i \leqslant T_D$) are not presented because averages differences are always below 10%. Within each subset of plots, the first, second and third rows correspond, always, to structures embedded $L = 40, 60$ and $80\,\text{m}$ respectively, while the five columns correspond to the points along the structure where this average difference is computed ($z/L = 0.00, 0.25, 0.50, 0.75$ and 1.00). In each plot, horizontal and vertical axes are the surrounding soil shear wave velocity (V_s) and the structure slenderness ratio (L/D), respectively.

A number of conclusions can be drawn from these results. The average errors obtained in the low-periods branch when using the rigid assumption is much larger than along the intermediate-periods branch, while they are generally below 10% in the high-periods branch (results not shown) for the values of the slenderness ratios (L/D) and wave propagation velocity (V_s) considered in this study. On the other hand, $z/L = 0.25$ and 1.00 are the depths for which computed discrepancies are smallest, while $z/L = 0.50$ tend to be the point for which errors are largest. In any case, discrepancies increase with the embedment length L of the structure, with softer soils and also, as expected, for more slender structures, although in many cases, and contrary to what was anticipated, the error is quite independent of the slenderness ratio. The discrepancies also tend to increase for hollow structures, but this is not always true and, in any case, the differences between the errors in the solid and hollow configurations are not significant, which allows to propose a criterion not dependent on this character.

Table 2 synthesizes the results presented in figures 9 and 10 with the aim of serving as a practical guide for helping to know if the hypothesis of infinite rigidity of a large buried structure (with the
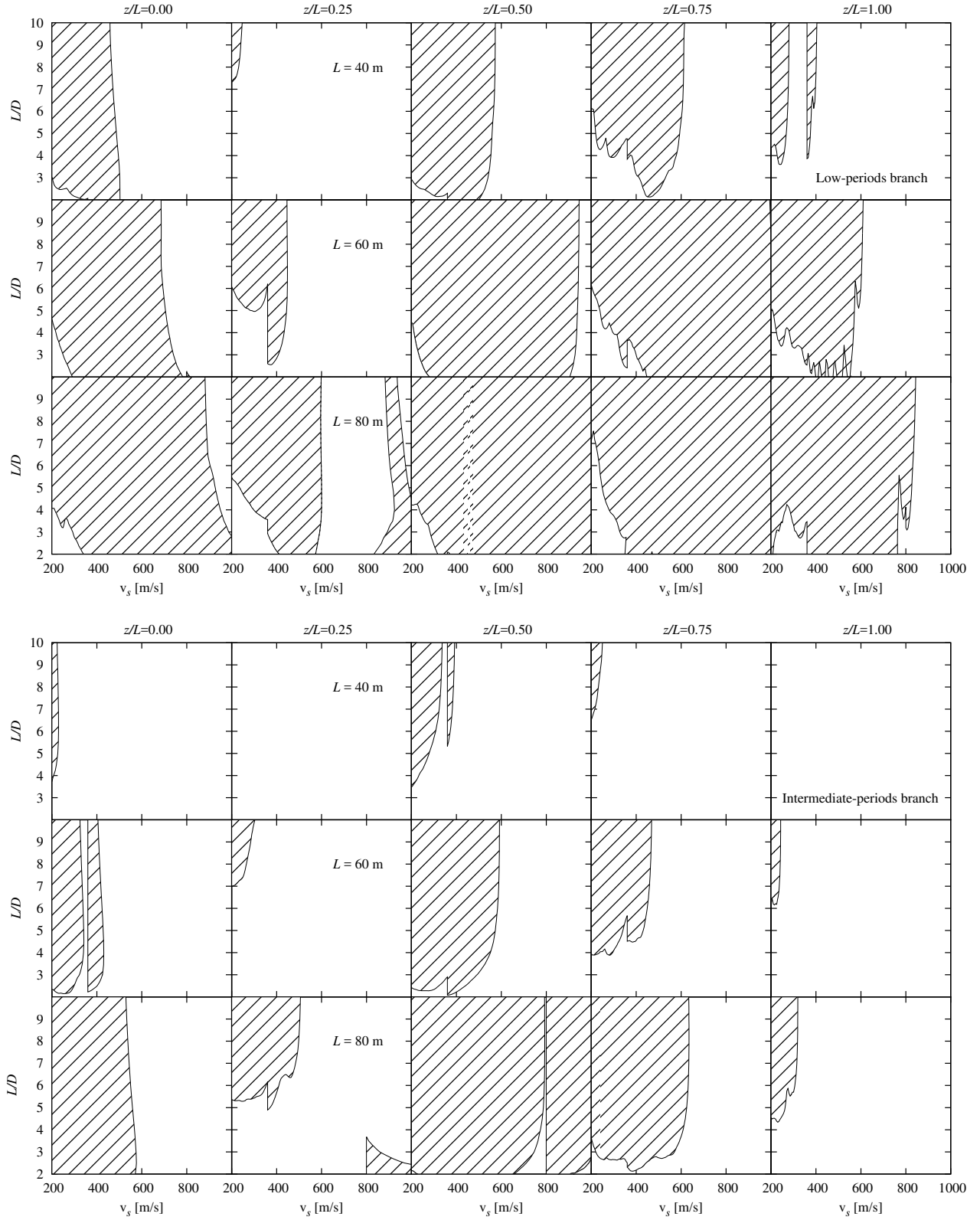
Figure 9: Filled surfaces represent the configurations (L/D and V_s values) for which $\bar{\epsilon} > 10\%$ at different depths z/L (columns) and for structures of embedment lengths of $L = 40$, 60 and 80 m (rows). Low-periods (top) and Intermediate-periods (bottom). Hollow structure ($\delta = 0.85$).
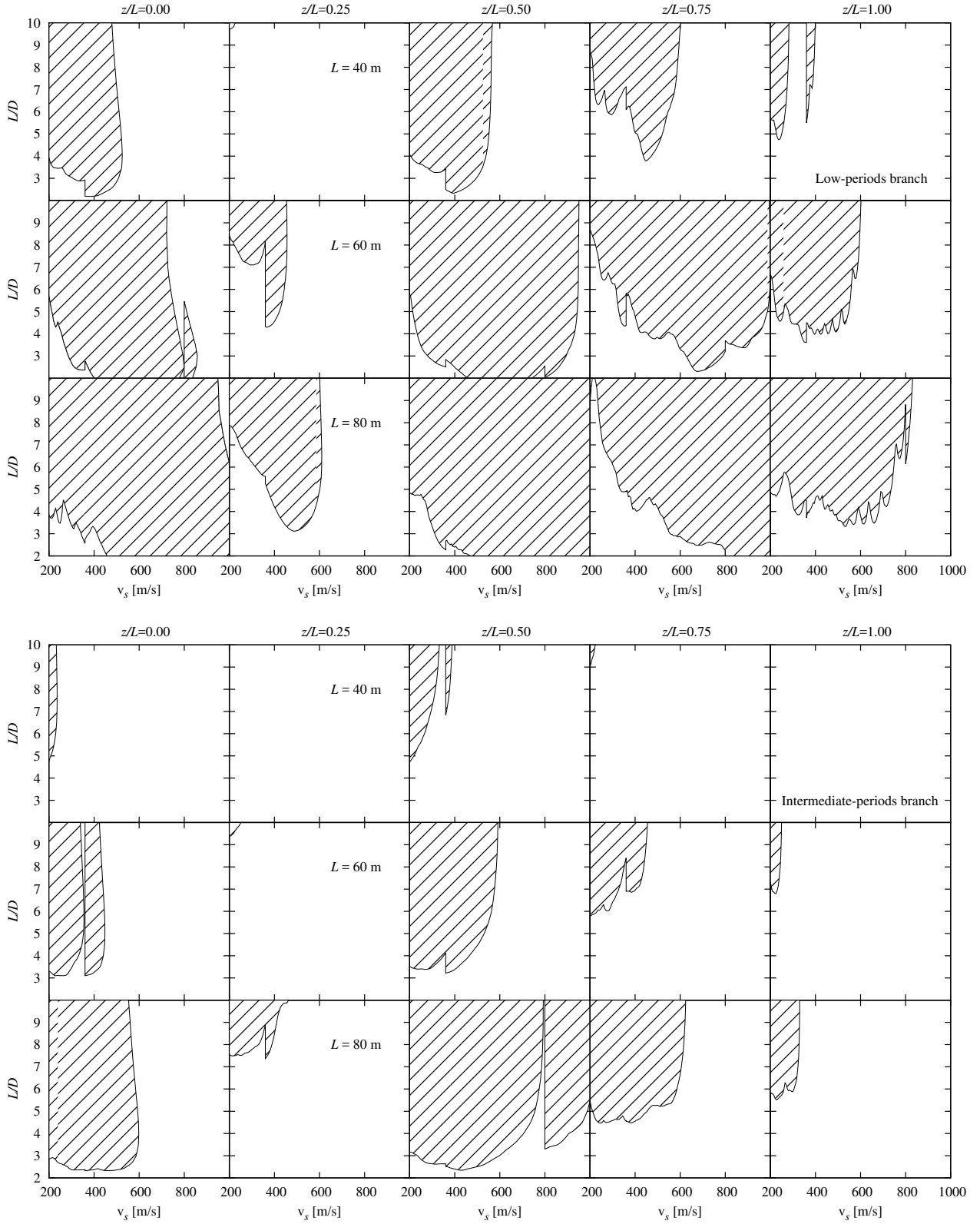
Figure 10: Filled surfaces represent the configurations (L/D and V_s values) for which $\bar{\epsilon} > 10\%$ at different depths z/L (columns) and for structures of embedment lengths of $L = 40$, 60 and 80 m (rows). Low-periods (top) and Intermediate-periods (bottom). Solid structure ($\delta = 0$).

14

mentioned safety margin of 10%) is applicable when evaluating its seismic response. The criterion is proposed only for the low- and intermediate-periods branches, as the rigid model is considered always valid for calculations in the high-period branch. As an application example, consider a structure with slenderness ratio $L/D = 7$ embedded in a soil characterized by a wave propagation velocity $V_s = 700\,\text{m/s}$ (ground type B). Following the criterion defined in table 2, using a rigid model for computing the response at $z/L = 0.25$ is always suitable for the embedment lengths studied herein. However, for a different wave velocity $V_s = 400\,\text{m/s}$ (even if it is the same ground type), the rigid body assumption is only valid if $L \leqslant 40\,\text{m}$ in the low-periods branch, or $L \leqslant 60\,\text{m}$ in the intermediate-periods branch.

Table 2: Conditions that should hold for considering the rigid assumption as valid for computing the spectral seismic response of a buried structure for each spectrum branch and depth of interest ($\bar{\epsilon}(z) \leqslant 10\%$)

	Low-periods branch	Intermediate-periods branch
$z/L = 0$	$L \leqslant 60$ and $\frac{V_s}{L} \geqslant 12$	$\frac{V_s}{L} \geqslant 7.5$
$z/L = 0.25$	$L \leqslant 40$ or $600 \leqslant V_s \leqslant 900\,\text{m/s}$	$L \leqslant 60$ or $-6 \leqslant \left(\frac{L}{D} - \frac{V_s}{85}\right) \leqslant 2$
$z/L = 0.50$	$L \leqslant 40$ and $V_s \geqslant 600\,\text{m/s}$	$L \leqslant 60$ and $\frac{V_s}{L} \geqslant 10$
$z/L = 0.75$	$L \leqslant 40$ and $V_s \geqslant 600\,\text{m/s}$	$L \leqslant 40$ or $\frac{V_s}{L} \geqslant 8$
$z/L = 1.00$	$\frac{V_s}{L} \geqslant 10$	$\frac{V_s}{L} \geqslant 4$

Contrary to what is commonly believed, it is therefore not possible to elucidate whether a buried structure behaves as rigid or not, based only on the slenderness ratio L/D. It is also necessary to take into account soil stiffness and embedment length, as both parameters are directly related to the variability of the seismic excitation along the buried structure. Besides, the depth of the point of study and the value of the period of interest can also influence the type of response.

If the criterion shown in table 2 needs to be simplified even further, it can be said that structures with slenderness ratios below 6 and embedment lengths below 20 m ($L/D < 6$ and $L < 20$ m) behaves always as a rigid solid, with independence of the stiffness of the soil. On the contrary, for increasing embedment lengths, soil stiffness becomes the main parameter, with structures behaving as not rigid for all type C and D soils, and most type B soils, for embedment lenghts of 40 m ($L = 40$ m).

6 Conclusions

This piece of research tries to contribute to answer to the following three questions: a) Is it possible to estimate the seismic response of a large buried structure, in terms of seismic motion, by using a model in which such structure is represented as a rigid body?, b) when does such simplifying assumption cease to be valid from an engineering point of view?, c) what simple engineering criterion can be proposed to determine the validity or not of the use of such simplified model?

In order to address these questions, a parametric study of the seismic response of buried structures was performed taking into account the more salient features of the problem: structural slenderness ratio, embedment length, soil stiffness, and structural typology (hollow or solid). The metodology used is based on the BDWF approach, previously verified by comparison against results obtained for the problem at hand using a more rigorous 3D multidomain boundary element model. Future developments of this analysis should study, for instance, the influence of the presence of soil layers or the influence of different types of non-linearities on the conclusions drawn from the linear-elastic model used in this paper.

The results are synthesized by computing and presenting average differences between the seismic spectral responses obtained from a model in which the structure is assumed as a rigid body, or with

its actual flexibility (i.e., the relative error made by assuming the hypothesis of infinity rigidity for the structure). That average error is computed separately for each of the branches of the acceleration response spectra defined in the Eurocode–8 [7], and for different depths along the structure. The hypothesis of infinity rigidity is assumed to be valid when such errors are below 10%.

The results show that the hypothesis of infinity rigidity for the structure is valid, independently of slenderness ratio or soil properties, for small embedment lengths or for natural frequencies of interest found along the branch of high periods of the elastic response spectra. For other situations, a specific criterion involving embedment length, soil stiffness and slenderness ratio is proposed for establishing when it is necessary to use models that consider the flexibility of the buried structure.

Acknowledgments

Appendix A

Dynamic soil reactions for plane strain case [23]:

$$K_x = \mu_s \left[S_x^r (a_o, \nu_s, \xi_s) + \mathrm{i}\, S_x^i (a_o, \nu_s, \xi_s) \right] = \frac{\pi}{4}\, \mu_s a_o^2\, T \tag{A.1a}$$

$$K_\theta = \mu_s\, D^2 \left[S_\theta^r (a_o, \nu_s, \xi_s) + \mathrm{i}\, S_\theta^i (a_o, \nu_s, \xi_s) \right] = \frac{\pi}{4}\, \mu_s\, D^2\, (1 + 2\xi_s \mathrm{i}) \left[a_o^* \frac{K_0 (a_o^*)}{K_1 (a_o^*)} + 1 \right] \tag{A.1b}$$

where the dimensionless frequency-dependent factor

$$T = -\frac{4K_1 (b_o^*)\, K_1 (a_o^*) + a_o^* K_1 (b_o^*)\, K_0 (a_o^*) + b_o^* K_0 (b_o^*)\, K_1 (a_o^*)}{b_o^* K_0 (b_o^*)\, K_1 (a_o^*) + a_o^* K_1 (b_o^*)\, K_0 (a_o^*) + a_o^* b_o^* K_0 (b_o^*)\, K_0 (a_o^*)} \tag{A.2}$$

being K_n the modified Bessel Functions of the second kind and order n with complex arguments:

$$a_o^* = \frac{a_o^* \mathrm{i}}{2\sqrt{1 + 2\xi_s \mathrm{i}}} \quad ; \quad b_o^* = \frac{a_o^* \mathrm{i}}{2\psi\sqrt{1 + 2\xi_s \mathrm{i}}} \quad \text{where} \quad \psi = \sqrt{\frac{2 (1 + \nu_s)}{1 - 2\nu_s}} \tag{A.3}$$

NOTE: The differences regarding this equations in Novak et al. [23] have to do with the dimensionless frequency ($a_o = \omega\, D/\mathrm{V}_s$) used in this work.

Appendix B

The exppressions of Veletsos and Verbič [33] for the impedance functions (rigid circular footing on a halfspace) applied in the bottom of structure:

$$\tilde{K}_j (a_o, \nu_s) = \sigma_j \left[k_j (a_o, \nu_s) + \mathrm{i}a_o c_j (a_o, \nu_s) \right] \quad ; \quad j = x, \theta \tag{B.1}$$

where k_j and c_j represent frequency-dependent stiffness and damping coefficients, approximated with the following expressions:

$$k_x = 1 \tag{B.2a}$$

$$c_x = a_1 \tag{B.2b}$$

$$k_\theta = 1 - b_1 \frac{(b_2 a_o)^2}{1 + (b_2 a_o)^2} - b_3 a_o^2 \tag{B.2c}$$

$$c_\theta = 2b_1 b_2 \frac{(b_2 a_o)^2}{1 + (b_2 a_o)^2} \tag{B.2d}$$

where a_1, b_1, b_2 and b_3 are coefficients that depend of ν_s and whose values are a_1=0.33, b_1=0.5, b_2=0.4 and b_3=0 (taken from Table I in Veletsos and Verbič [33] for $\nu_s = 1/3$). Finally, σ_j is the dimensionless static stiffness that take the following expressions for swaying and rocking problems:

$$\sigma_x = \frac{4}{2 - \nu_s} \quad ; \quad \sigma_\theta = \frac{1}{3(2 - \nu_s)} \tag{B.3}$$

NOTE: In this appendix also the differences regarding this equations and coefficients in Veletsos and Verbič [33] have to do with the dimensionless frequency ($a_o = \omega D/V_s$) used in this work.

References

[1] G. Anoyatis and A. Lemnitzer. Dynamic pile impedances for laterally-loaded piles using improved Tajimi and Winkler formulations. *Soil Dyn Earthq Eng*, 92:279–297, 2017.

[2] S. Argyroudis, G. Tsinidis, F. Gatti, and K. Pitilakis. Effects of SSI and lining corrosion on the seismic vulnerability of shallow circular tunnels. *Soil Dyn Earthq Eng*, 98:244–256, 2017.

[3] A. Bahrami and H. Nikraz. Generalized Winkler support properties for far field modeling of larerally vibrating piles. *Soil Dyn Earthq Eng*, 92:684–691, 2017.

[4] E. Buckingham. On physically similar systems. Illustrations of the use of dimensional equations. *Phys Rev*, 4:345–376, 1914.

[5] R. Conti, M. Morigi, and G. M. B. Viggiani. Filtering effect induced by rigid massless embedded foundations. *Bull Earthq Eng*, 15(3):1019–1035, 2017.

[6] F. Elsabee, J. P. Morray, and J. M. Roesset. Dynamic behavior of embedded foundations. *Research Report R77-33, MIT, Cambridge MA*, 1977.

[7] Eurocode-8. *Design of Structures for Earthquake Resistance. Part 1: General Rules, Seismic Actions and Rules for Buildings.* European Standard EN-1998-1, CEN/TC 250: Brussels, 2003.

[8] R. Flores-Berrones and R. V. Whitman. Seismic response of end-bearing piles. *J Geotech Eng - ASCE*, 108(4):554–569, 1982.

[9] G. Gazetas and R. Dobry. Horizontal response of piles in layered soils. *J Geotech Eng - ASCE*, 110(1):20–40, 1984.

[10] N. Gerolymos and G. Gazetas. Winkler model for lateral response of rigid caisson foundations in linear soil. *Soil Dyn Earthq Eng*, 26:347–361, 2006.

[11] S. M. Hasheminejad and S. Kazemirad. Dynamic response of an eccentrically lined circular tunnel in poroelastic soil under seismic excitation. *Soil Dyn Earthq Eng*, 28:277–292, 2008.

[12] G. D. Hatzigeorgiou and D. E. Beskos. Soil–structure intection effects on seismic inelastic analysis of 3-D tunnels. *Soil Dyn Earthq Eng*, 30:851–861, 2010.

[13] E. Kausel, R. V. Whitman, J. P. Morray, and F. Elsabee. The spring method for embedded foundations. *Nucl Eng Des*, 48:377–392, 1978.

[14] M. Kavvadas and G. Gazetas. Kinematic seismic response and bending of free heads piles in layered soil. *Geotechnique*, 43(2):207–222, 1993.

[15] K. C. Lin, H. H. Hung, J. P. Yang, and Y. B. Yang. Seismic analysis of underground tunnels by the 2.5D finite/infinite element approach. *Soil Dyn Earthq Eng*, 85:31–43, 2016.

[16] O Maeso, J J Aznárez, and J Domínguez. Effects of space distribution of excitation on seismic response of arch dams. *J Eng Mech (ASCE)*, 128 (7):759–768, 2002.

[17] O Maeso, J J Aznárez, and J Domínguez. Three-dimensional models of reservoir sediment and effects on the seismec response of arch dams. *Earthq Eng Struct Dyn*, 33:1103–1123, 2004.

[18] N. Makris. Soil-pile interaction during the passage of Rayleigh waves: an analytical solution. *Earthq Eng Struct Dyn*, 23(2):153–167, 1994.

[19] N. Makris and G. Gazetas. Displacement phase differences in a harmonically oscillating pile. *Geotechnique*, 23(1):135–150, 1993.

[20] G. Mylonakis. Elastodynamic model for large diameter end bearing shafts. *Soils Found*, 41(3):31–44, 2001.

[21] G. Mylonakis. Simplified model for seismic pile bending al soil layer interfaces. *Soils Found*, 41(4):47–58, 2001.

[22] M. Novak. Dynamic stiffness and damping of piles. *Can Geotech J*, 11(4):574–598, 1974.

[23] M. Novak, T. Nogami, and F. Aboul-Ella. Dynamic soil reactions for plane strain case. *J Eng Mech - ASCE*, 104(EM4):953–959, 1978.

[24] D. Park, M. Sagong, D-Y Kwak, and C-G Jeong. Simulation of tunnel response under spatially varying ground motion. *Soil Dyn Earthq Eng*, 29:1417–1424, 2009.

[25] M. Saitoh and H. Watanabe. Effects of flexibility on rocking impedance of deeply embedded foundation. *J Geotech Geoenviron Eng*, 130(4):435–445, 2004.

[26] A. Santana, J. J. Aznárez, L. A. Padrón, and O. Maeso. A BEM-FEM model for the dynamic analysis of building structures founded on viscoelastic or poroelastic soils. *Bull Earthq Eng*, 14(1):115–138, 2016.

[27] M. Shadlou and S. Bhattacharya. Dynamic stiffness of monopiles supporting offshore wind turbine generators. *Soil Dyn Earthq Eng*, 88:15–32, 2016.

[28] H. Tajimi. Dynamic analysis of a structure embedded in a elastic stratum. *Proc 4th World Conf on Earthq Eng. Santiago de Chile*, pages 53–69, 1969.

[29] S. P. Timoshenko. On the correction for shear of the differential equation for transverse vibrations of prismatic bars. *Philosophical Magazine Series 6*, 41(245):744–746, 1921.

[30] S. P. Timoshenko. On the transverse vibrations of bars of uniform cross-section. *Philosophical Magazine Series 6*, 43(256):125–131, 1922.

[31] Varun, D. Assimaki, and G. Gazetas. A simplified model for lateral response of large diameter caisson foundations: Linear elastic formulation. *Soil Dyn Earthq Eng*, 29(2):268–291, 2009.

[32] J. Vega, J. J. Aznárez, A. Santana, L. A. Padrón, E. Alarcón, J. J. Pérez, and O. Maeso. On soil-structure interaction in large non-slender partially buried structures. *Bull Earthq Eng*, 11:1403–1421, 2013.

[33] A. S. Veletsos and B. Verbič. Vibration of viscoelastic foundations. *Earth Eng Struct Dyn*, 2(1):87–102, 1973.